Hydromagnetic waves in a cylindrical plasma: an experiment

By D. F. JEPHCOTT AND P. M. STOCKER
Culham Laboratory, Berkshire

(Received 7 April 1962)

In a previous paper (Woods 1962) a theory is presented which leads to a general dispersion relation for hydromagnetic waves in a dissipative plasma contained in a cylindrical tube. In the present paper experimental observations are compared with the predictions of this theory.

An experiment is described in which torsional hydromagnetic waves are excited in a gas discharge. Measurements of the wave velocity and damping are compared with solutions of the dispersion equation which are computed from measured values of the plasma parameters. The results are consistent with the theory, and good numerical agreement is obtained by assuming a loss of particles to the tube walls. There is evidence of a cut-off in wave propagation in the region of ion cyclotron resonance.

1. Introduction

Theories of hydromagnetic wave phenomena have been extensively developed by a number of authors (see De Silva 1961 for bibliography) but only a limited amount of experimental evidence is available to support these theories. Hydromagnetic waves in liquid metals were studied by Lundquist (1949) and Lehnert (1954), and the excitation of hydromagnetic waves in plasmas was reported independently by Allen *et al.* (1959) and by Jephcott (1959). Recent experimental work has been described by Hooke *et al.* (1961), Nagao *et al.* (1960), Sinelnikov *et al.* (1961) and Wilcox *et al.* (1961).

In this paper we describe the investigation of torsional hydromagnetic waves in a gas discharge plasma. The waves are excited by a method similar to that used by Allen *et al.* Conditions are such that the wave motion is heavily damped by resistive dissipation in the plasma, the ratio of the wave frequency ω to the ion cyclotron frequency ω_{ci} is varied between 0·1 and 1, and ω is less than the frequency ω_{ni} of neutral atom collisions with positive ions. In analysing the experimental results we use the theory of Woods (1961, 1962).

2. Experimental method

2.1. *Apparatus*

The plasma is produced by a gas discharge in a cylindrical quartz tube, of 10 cm bore and 200 cm long, fitted with stainless-steel disk electrodes at each end and with a co-axial return conductor. This assembly (see figure 1) is mounted in a solenoid connected to a 200 kJ capacitor bank which provides an axial magnetic field up to 16 kG with a rise time of 1 ms. The tube is supplied with a continuous flow of argon or neon at a pressure of 50μ Hg. A 12 kJ capacitor bank switched across the end electrodes initiates the discharge; the current rises to a peak of 12 kA in 120 μs and is timed to coincide with the maximum of the axial magnetic field. Both capacitor banks are short-circuited

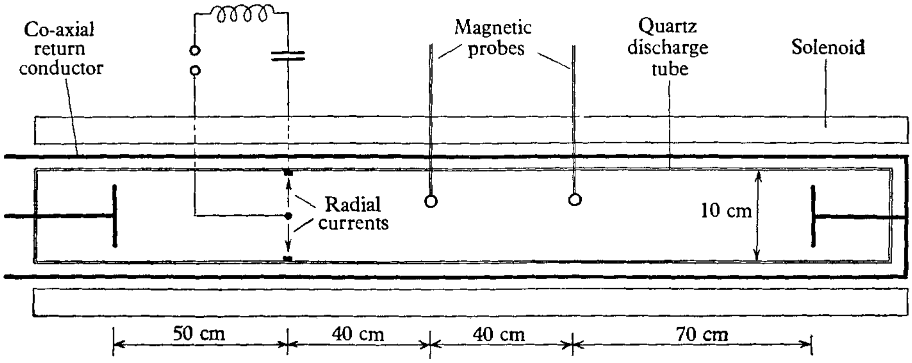

FIGURE 1. Diagram of apparatus (not to scale).

at the time of maximum current; the magnetic field and gas current then decay exponentially. The essential part of the experiment is carried out in the first 10 to 20 μs of the exponential decay, during which the magnetic field and gas current decrease by less than 0·01 %.

The following account is concerned with this 'steady state' phase.

2.2. *Wave excitation*

The hydromagnetic wave is excited in a region 50 cm from one end of the tube, where the plasma is free from any non-uniformity and impurities associated with the main electrodes. At the beginning of the steady phase of the discharge a 50 J capacitor, with a suitable inductance in series, is discharged between a ball electrode on the tube axis and a concentric ring electrode mounted on the inner wall of the discharge tube (see figure 1); this circuit is allowed to oscillate freely. Inductances are chosen to give oscillation frequencies of either 125 or 250 kc/s, the peak current is about 1 kA, and the exciter circuit, including the plasma impedance, has a Q-value of about 10. The oscillating radial current in the plasma is perpendicular to the steady axial magnetic field and therefore produces local torsional oscillations, which propagate along the tube as an $m = 0$ slow wave. The wave can be treated as essentially monochromatic since Fourier analysis of the damped oscillation of the exciter circuit shows that the component frequencies lie in a band with a half-width of only 6 kc/s.

2.3. *Wave detection*

The wave is detected by two magnetic probe coils, 5 mm in diameter, spaced at 40 cm intervals from the exciter electrodes and 2·5 cm from the tube axis. The phase velocity, V_{ph}, is found from the time delay between the two probe signals, and the decay length, Z_0 (i.e. the e-folding length) from their relative amplitudes. In a typical experiment the wave amplitude is in the range 10 to 100 G. Figure 2(*a*) shows an oscillogram of the probe signals, which are unfiltered and unintegrated, and figure 2(*b*) shows three exposures on the same film to illustrate the repeatability in successive discharges. The regularity of the signals demonstrates the absence of gross instabilities in the discharge; the high frequency 'hash' at the start of the traces comes from a spark gap in the exciter circuit. There is no evidence of interference from waves reflected by the end electrodes.

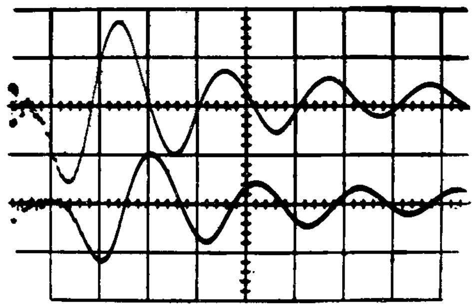

(*a*)

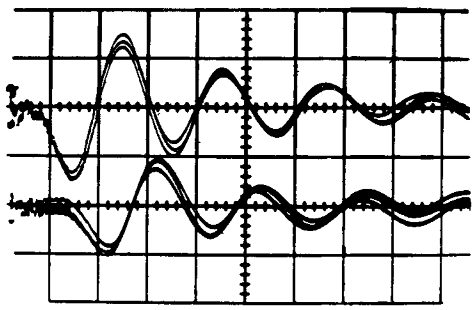

(*b*)

FIGURE 2. (*a*) Magnetic probe signals; argon, 125 kc/s. (*b*) Three traces overlaid to show repeatability.

To study the behaviour of the wave at frequencies, ω, close to the ion cyclotron frequency, ω_{ci}, we investigated a range of experimental conditions over which the ratio ω/ω_{ci} varies from about 0·1 to 1. In practice, it is simpler to vary ω/ω_{ci} $(= \omega m_i/eB_0)$ by changing B_0 rather than by changing ω. At one magnetic field strength near the lower end of the experimental range ω_{ci} is equal to ω, and ion cyclotron resonance is approached as the field is reduced towards this resonance value. Propagation of the hydromagnetic wave can be observed only with B_0 above the resonance value (i.e. with $\omega < \omega_{ci}$). As ω/ω_{ci} increases to unity the signal-to-noise ratio becomes too low for V_{ph} and Z_0 to be measured, and there are no detectable signals when $\omega/\omega_{ci} > 1$.

2.4. *Plasma properties*

To compare experimental measurements of V_{ph} and Z_0 with theory we must know the numerical values of the plasma parameters which appear in the dispersion equation, i.e. the ion and neutral atom number densities n_i and n_n, the electrical conductivities $\sigma_\parallel$ and $\sigma_\perp$, and ω_{in} the collision frequency of positive ions with neutral atoms. We must also examine the validity of the theoretical assumption that the tube is uniformly filled with plasma.

The properties of the argon plasma are described below.

(*a*) Magnetic probe measurements show that the discharge current density decreases with increasing tube radius. Between $r = 0$ and $r = 4{\cdot}5$ cm the current density falls by 5 % and then decreases sharply to zero at the tube walls. The plasma can thus be regarded as a hot core surrounded by an annular boundary layer of cool plasma about 5 mm thick. With axial magnetic fields below 4 kG the discharge has a tendency to pinch; no quantitative experiments were carried out in this region.

(*b*) From probe measurements of the axial electric field and current density, the average plasma conductivity including that of the boundary layer is $\sigma_\parallel = 65 \pm 5\ \Omega^{-1}\,\text{cm}^{-1}$, and we assume $\sigma_\perp = \frac{1}{2}\sigma_\parallel$ (see Spitzer 1956). The conductivity in the hot core is $75 \pm 5\ \Omega^{-1}\,\text{cm}^{-1}$ and the corresponding electron temperature is $T_e = 1{\cdot}9 \pm 0{\cdot}1$ eV. These figures are for magnetic fields above 4 kG.

(*c*) A Langmuir double probe (Johnson & Malter 1950) was used to measure the electron temperature T_e and the ion number density n_i at the positions of the two magnetic probes which detect the wave and at different radii. A scatter of ± 10 % in these measurements was sufficient to prevent the detection of any consistent spatial variations in the hot core. The results were averaged, giving $n_i = 1{\cdot}0 \pm 0{\cdot}1 \times 10^{15}\,\text{cm}^{-3}$, and $T_e = 2{\cdot}3 \pm 0{\cdot}1$ eV which agrees with the figure calculated from $\sigma_\parallel$ to within 20 %. The Langmuir probe results are independent of the magnetic field strength above 4 kG. The number density of neutral atoms, n_n, was not measured, but since the initial particle density is $1{\cdot}8 \times 10^{15}\,\text{cm}^{-3}$ we can expect n_n to be equal to, or less than, $8 \times 10^{14}\,\text{cm}^{-3}$ depending on whether or not particles are lost to the tube walls during the discharge.

(*d*) An estimate of the ion temperature, T_i, was obtained from the Doppler width of an argon spectrum line, measured by crossing a Fabry–Perot interferometer with a prism spectrograph (Turnbull *et al.* 1955). The A II line, $\lambda = 4609$ Å, was used because of its negligible Stark broadening. No time resolution was included in this measurement, so the value obtained, $T_i = 1{\cdot}7 \pm 0{\cdot}2$ eV, is an effective average over the duration of the discharge pulse.

(*e*) The ion-neutral collision frequency, ω_{in}, is given approximately by $\omega_{in} = n_n \sigma_m v_i$, where σ_m is the momentum transfer cross-section and v_i is the mean thermal velocity of ions.

Hornbeck (1951) has given the value of a hard sphere collision cross-section, σ_i, for A^+ in A based on measurements of ion drift velocities at high E/p. Since the range of drift velocities includes the mean thermal velocities of the ions in our experiment, we take Hornbeck's σ_i as a measure of the σ_m which we require. Using $\sigma_m = 1{\cdot}3 \times 10^{-14}\,\text{cm}^2$ and $T_i = 1{\cdot}7$ eV, we have $\omega_{in} = n_n \times 4{\cdot}5 \times 10^{-9}\,\text{sec}^{-1}$. A neutral atom collides with positive ions with a frequency $\omega_{ni} \sim n_i \sigma_m v_i$. If $n_i = 10^{15}\,\text{cm}^{-3}$, then $\omega_{ni} = 4{\cdot}5 \times 10^{6}\,\text{sec}^{-1}$; this is greater than the wave frequency, and neutral atoms will therefore tend to take part in the wave motion.

(*f*) The magnetic probes which are used to detect the hydromagnetic wave also pick up random noise from the discharge with frequencies of the order of 100 kc/s. By using axial magnetic fields above 3 or 4 kG the noise amplitude can be limited to an order of magnitude less than the wave amplitude over most of the experimental range.

For the experimental plasma parameters given above, the pressure and viscosity terms in the dispersion relation (equation (27) of Woods 1962) are negligible. The plasma pressure is about three orders of magnitude less than the magnetic field pressure, and the theoretical contribution of viscosity to the wave decay is two orders of magnitude less than that of the plasma resistivity. The dispersion equation therefore reduces to Woods' equation (60).

A few experiments were carried out using neon instead of argon, but the plasma diagnostics for this case are incomplete. The noise level in the neon discharge was too high to permit satisfactory Langmuir probe measurements, and the ion temperature was not measured. The radial variation of current density was similar to that in argon and there was no significant difference in the electrical conductivities of the two plasmas.

3. Results

3.1. *Wave mode*

The wave mode is examined by moving a magnetic probe coil across the tube diameter. Figure 3 shows the observed radial variation of $B_{1\theta}$, the azimuthal component of the wave magnetic field, for a 125 kc/s wave in argon. Each

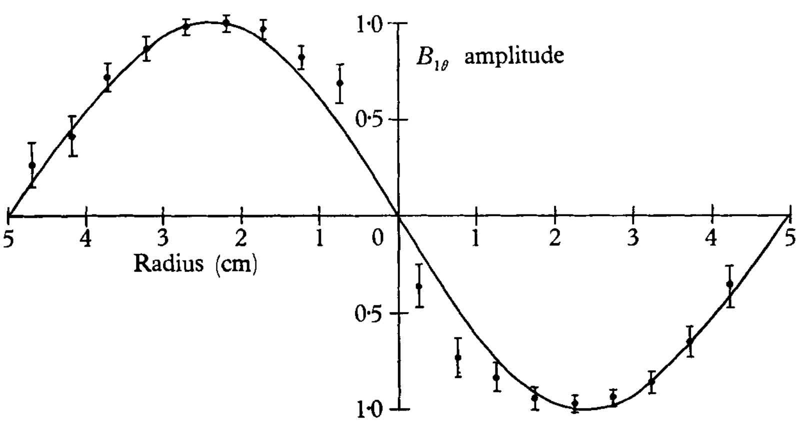

FIGURE 3. Observed amplitude of wave $B_{1\theta}$ as $f(r)$ compared with $J_1(k_c r)$; argon 125 kc/s.

experimental point represents the average of 10 successive measurements and the probable error is indicated by vertical bars. The measurements are compared with the solid curve which represents the first-order Bessel function $J_1(k_c r)$, with the first zero occurring where r is equal to the tube radius. The observed amplitudes and the Bessel function are normalized to have a maximum of unity. At radii greater than about 1 cm the agreement is within the experimental error, indicating that the wave consists largely of the lowest-order $m = 0$ mode with $B_{1\theta} = 0$ at the tube walls. Discrepancies, increasing to about 50 % near the tube axis, might be due to the presence of higher-order $m = 0$ modes with relatively small amplitudes. Such modes could arise as a result of the radia variation in exciter current density.

Small B_{1r} and B_{1Z} signals can be detected experimentally but their random character suggests that they arise as a result of turbulence in the plasma. The theory predicts that, because of the dominant effect of dissipation, B_{1r} and B_{1Z} should be about two orders of magnitude less than $B_{1\theta}$ in the range of the experimental measurements.

The boundary conditions for an insulating tube, given in Woods's equations (78) and (79) cannot both be satisfied by a torsional wave alone. However, the dispersion equation (60) is quadratic in α and two waves can therefore occur with different radial wave-numbers arising from the two roots in α. One of these waves is torsional, with magnetic field components given in equation (80), the second is a compressional wave with field components given in equation (81). The presence of this second wave accompanying the first is necessary to satisfy the boundary conditions, but since B_{1r} and B_{1Z} in the torsional wave are small, the necessary amplitude of the compressional wave must also be small and can be neglected in the discussion.

A further complication in the experiment is the presence of a cool boundary layer, in which the plasma viscosity and gradients in density and conductivity may give rise to boundary effects not considered in the theory.

3.2. *Comparison of results with theory*

Woods's dispersion equation (60) has been solved numerically to give V_{ph} and Z_0 as functions of B_0. Using first the values $n_i = 10^{15}\ \text{cm}^{-3}$, $n_n = 8 \times 10^{14}\ \text{cm}^{-3}$, and $\sigma_{\parallel} = 65\ \Omega^{-1}\ \text{cm}^{-1}$, we obtain solutions for a 125 kc/s wave in argon; these solutions are plotted as dashed curves in figures 4 and 5. In figure 4 most of the experimental points lie above the dashed theoretical curve for V_{ph}, indicating that the total mass involved in the observed wave motion is less than that implied by the above values of n_i and n_n. Also, the theoretical minimum in V_{ph} at 7 kG is not observed experimentally; this minimum moves to higher magnetic fields as the number of neutral atoms moving with the wave increases. The inference is that $8 \times 10^{14}\ \text{cm}^{-3}$ is too high a value for n_n. In figure 5, the decay lengths computed with $n_n = 8 \times 10^{14}\ \text{cm}^{-3}$ are also lower than the experimental points. This is to be expected since the decay length and phase velocity are linked by the decay time $\tau\ (= Z_0/V_{ph})$ which is largely determined by $\sigma_{\parallel}$ and ω/ω_{ci}.

Thus the discrepancies in V_{ph} and Z_0 can both be attributed to the use of too high a value of neutral atom density in computing the dispersion equation solutions. We therefore adopted a fitted parameter method to find the value of n_n which gives the best agreement between theory and experiment. The solid curves in figures 4 and 5 were obtained by taking $n_n = 1{\cdot}5 \times 10^{14}\ \text{cm}^{-3}$, which gives agreement almost within the probable experimental error (indicated by vertical bars).

Experimental results for a 125 kc/s wave in neon are shown in figures 6 and 7 with the argon results included for comparison; the resonance fields for neon and argon are indicated by arrows. Using Hornbeck's cross-section for Ne^+ in

Ne, $\sigma_m = 6{\cdot}5 \times 10^{-15}\,\mathrm{cm}^2$, the best fit between experiment and the dispersion equation solutions is obtained with $n_i = 5 \times 10^{14}\,\mathrm{cm}^{-3}$ and $n_n = 5 \times 10^{14}\,\mathrm{cm}^{-3}$. In this case n_i was not measured independently but determined as a second fitted parameter, and the ion temperature was assumed to be equal to that

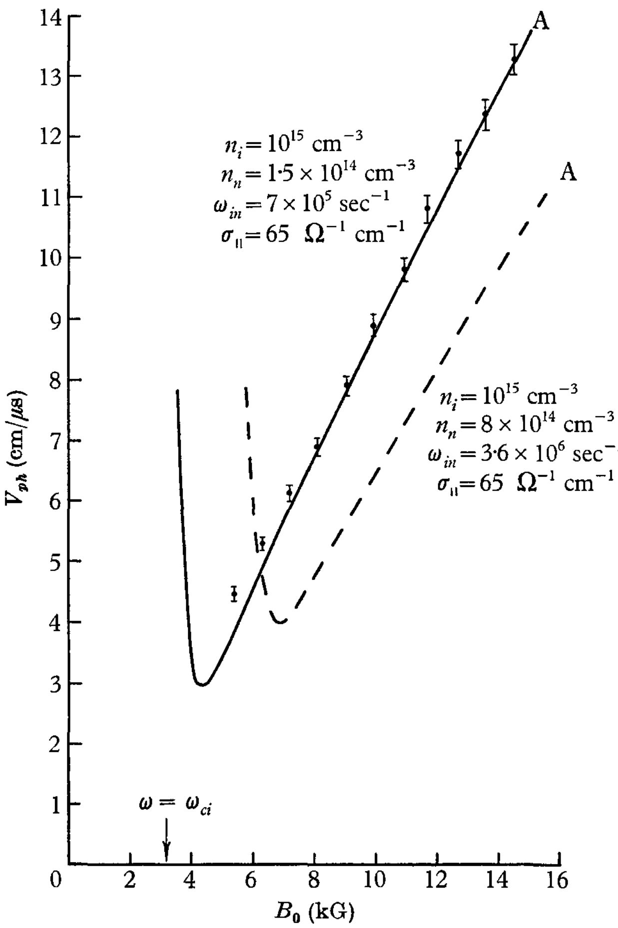

FIGURE 4. Measurements of V_{ph} as $f(B_0)$; argon, 125 kc/s. Curves represent computed solutions of dispersion equation.

measured for argon. Thus there is a larger margin of error in our numerical interpretation of the neon results, but they support the general picture provided by the argon results.

For both gases we obtain the best agreement between theory and experiment by assuming that over one-third of the particles initially in the tube are lost to the walls during the 120 μs rise-time of the discharge pulse. Simple collisional diffusion processes in a quiescent plasma are insufficient to account for such a large loss rate, but turbulence in the plasma may cause enhanced diffusion similar to the 'pump-out' phenomenon observed in Stellarator devices (Ellis *et al.* 1960). Positive ions or fast neutral atoms absorbed by the tube walls would be re-emitted as slow neutral atoms which would diffuse only a few millimetres

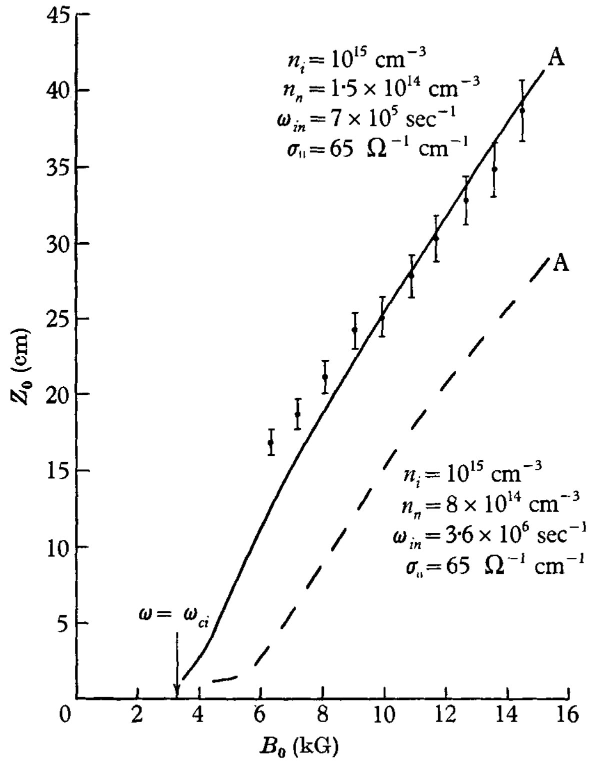

FIGURE 5. Measurements of Z_0 as $f(B_0)$; argon, 125 kc/s. Curves represent computed solutions of dispersion equation.

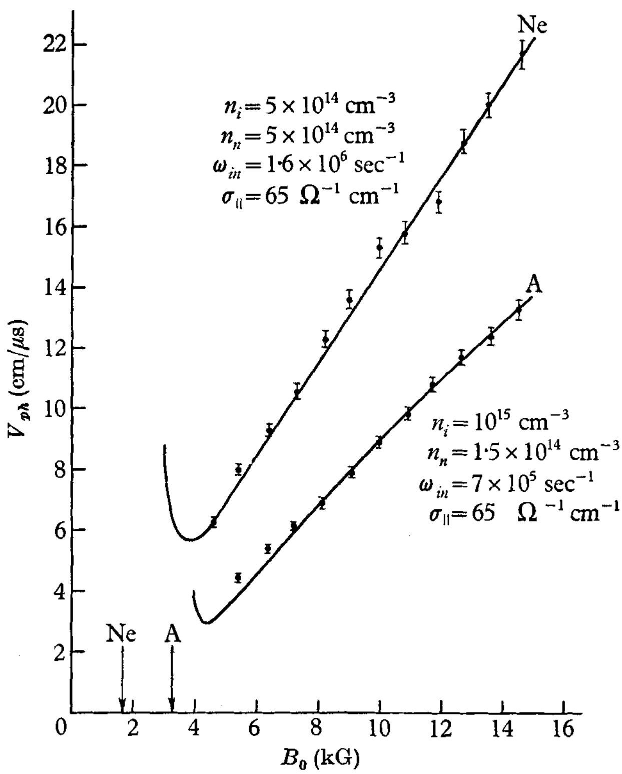

FIGURE 6. V_{ph} in neon and argon, 125 kc/s.

in the time available. This process may explain the formation of the cool boundary layer and the reduction in neutral atom density in the hot core.

The behaviour of the wave in the region of ion cyclotron resonance is modified by the effects of finite conductivity and ion-neutral collisions. In the simple case of a fully ionized plasma with infinite conductivity, the theory shows that the plasma velocity falls smoothly to zero as B_0 is decreased towards the

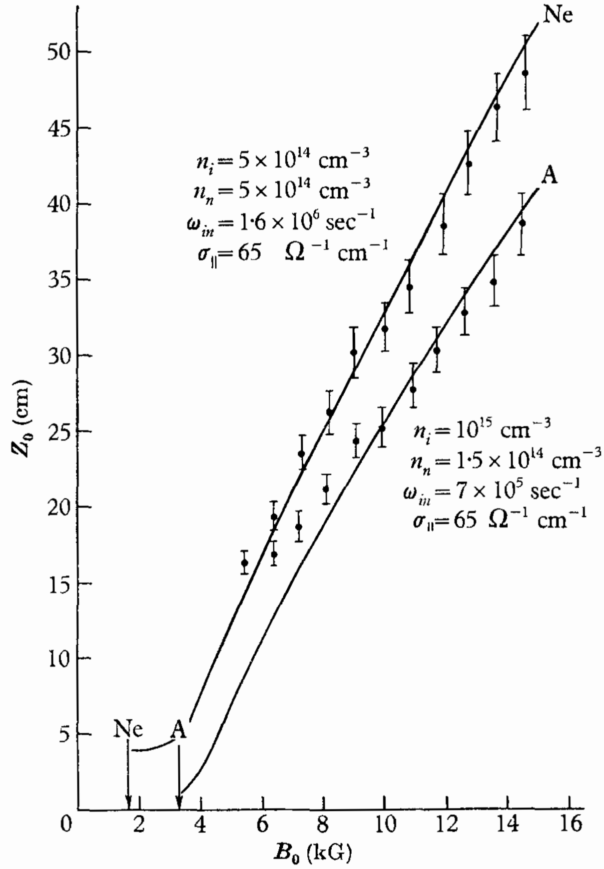

FIGURE 7. Z_0 in neon and argon, 125 kc/s.

resonance field B_R ($= \omega m_i/e$) and the decay length drops sharply from infinity to zero at $B_0 = B_R$. The inclusion of finite conductivity and the collision term in the dispersion equation reduces the sharpness of the resonance as indicated by the theoretical curves. V_{ph} now has a minimum value at a magnetic field strength which is dependent on the degree of coupling between ions and neutral atoms, and Z_0 decreases steadily to a small but finite value at $B_0 = B_R$. Experimentally we find that as B_0 is decreased towards B_R the magnetic probe signals become comparable with the background noise, and repeatable measurements of V_{ph} and Z_0 are no longer obtained. However, the presence of the wave can still be detected in this region until we reach a field strength, B_{min}, below which the probe signals are completely obscured by background noise. Within limits set by the noise level, B_{min} should be an approximate measure of the resonance field B_R. Table 1 compares the observed values of B_{min} with B_R.

In argon, $B_{min} = B_R$ to within 10% and the 250 kc/s wave in particular appears to have a sharp cut-off at B_R. In neon the background noise is somewhat greater and $B_{min} \sim 2B_R$.

Gas	Frequency (kc/s)	B_{min} (kG)	B_R (kG)
Argon	125	3·6	3·3
	250	6·6	6·6
Neon	125	3·2	1·65
	250	4·5	3·3

TABLE 1

4. Conclusions

The accuracy of the experimental results is limited by the difficulties of producing a reasonably quiescent uniform plasma and of measuring the plasma parameters which affect the wave motion. Measurements of the phase velocity and decay length are consistent with the theory and, by assuming a loss of particles to the tube walls, we can obtain agreement almost within the probable experimental error, the discrepancies at the worst points being less than 20%.

Wave propagation is never observed at frequencies greater than the ion cyclotron frequency, indicating a cut-off in the region of ion cyclotron resonance.

The experiment shows that hydromagnetic waves can provide a useful tool for diagnostics in plasmas which are permeated by a magnetic field.

The authors are grateful for the advice of Dr R. J. Bickerton, and for the experimental assistance of Mr R. A. Hardcastle and Mr A. I. Kilvington.

REFERENCES

ALLEN, T. K. *et al.* 1959 *Phys. Rev. Letters*, **2**, 383.
DE SILVA, A. W. 1961 *Ph.D. Thesis, Univ. California Rad. Lab.* Rep. no. 9601.
ELLIS, R. A. *et al.* 1960 *Phys. Fluids*, **3**, 468.
HOOKE, W. M. *et al.* 1961 *Phys. Fluids*, **4**, 1131.
HORNBECK, J. A. 1951 *Phys. Rev.* **84**, 615.
JEPHCOTT, D. F. 1959 *Nature, Lond.*, **183**, 1652.
JOHNSON, E. O. & MALTER, L. 1950 *Phys. Rev.* **80**, 58.
LEHNERT, B. 1954 *Phys. Rev.* **94**, 815.
LUNDQUIST, S. 1949 *Nature, Lond.*, **164**, 145.
NAGAO, S. *et al.* 1960 *J. Phys. Soc. Japan*, **15**, 735.
SINELNIKOV, K. D. *et al.* 1961 *Salzburg Conference*, paper no. CN–10/231.
SPITZER, L. 1956 *Physics of Fully Ionized Gases*. New York: Interscience Publishers Inc.
TURNBULL, A. H. *et al.* 1955 *A.E.R.E.* GP/R1793.
WILCOX, J. M. *et al.* 1961 *Phys. Fluids*, **4**, 1506.
WOODS, L. C. 1961 *Culham Laboratory Report* CLM-R13.
WOODS, L. C. 1962 *J. Fluid Mech.* **13**, 570.